Dawsonite-Type Precursors for Catalytic Al, Cr, and Fe Oxides: Synthesis and Characterization

Asma A. Ali,[†] Muhammad A. Hasan,[†] and Mohamed I. Zaki*[,‡]

Chemistry Department, Faculty of Science, Kuwait University, P.O. Box 5969, Safat 13060, Kuwait, and Chemistry Department, Faculty of Science, Minia University, El-Minia 61519, Egypt

Received August 24, 2005

Preparation of dawsonite-type compounds, $NH_4M(CO_3)(OH)_2$, was attempted for M = Al, Cr, or Fe, using a hydrothermal method under various basicity and thermal conditions. Crystalline structure and chemical composition verification studies, employing X-ray diffractometry, infrared spectroscopy, and elemental analyses, revealed that a successful preparation is critically dependent on the availability of $MO(OH)^-$ and HCO_3^- reaction species, which is facilitated at pH value in the vicinity of 10 and temperature ≤100 °C. Accordingly, it was possible to prepare dawsonite-type compounds for Al and Cr, but not for Fe. In the latter case, the sparingly soluble FeOOH compound was the eventual product. Thermal analyses of the hydrothermal products helped define the temperature regime at which they decompose into the corresponding M(III)-oxides. Bulk and surface characterization studies of the oxides thus produced revealed that dawsonite-type compounds are feasible precursors for catalytic-grade Al_2O_3 and Cr_2O_3.

Introduction

Dawsonite (*denoted* Dw) is a mineralogical nomenclature meant to specifically indicate naturally occurring sodium hydroxyaluminocarbonate, $NaAl(CO_3)(OH)_2$,[1] whose material bulk is organized in crystals of orthorhombic structure [space group *Imma*, with $a = 6.759$ Å, $b = 5.585$ Å, $c = 10.425$ Å, $Dm = 2.436$, and $dx = 2.431$ g/cm^3 for $Z = 4$ formula units].[2] It consists of edge-sharing $AlO_2(OH)_4$ and $NaO_4(OH)_2$ octahedra, with each CO_3 group (regular) being attached to two adjacent $AlO_2(OH)_4$ octahedra and two distorted $NaO_4(OH)_2$.[2] Hydrogen bonding occurs between the Al chain and the CO_3 group, strengthening the Al + Na three-dimensional framework.[2] However, sodium aluminum dawsonite (NaAlDw) is just a member of a large class of analogous (dawsonite-type) synthetic and natural compounds that are nominally described by the general chemical formula $AM(CO_3)_x(OH)_y$, where "A" is an alkali (K^+ or NH_4^+) or alkaline earth (Mg^{2+}, Ca^{2+}, or Ba^{2+}) metal ion and "M" is favorably a trivalent transition or nontransition metal ion,[1,3] or by $BM(CO_3)_x(OH)_y$, where "B" is a divalent transition metal ion (Ni^{2+} or Cu^{2+}).[1,3] Similar hydroxymetalocarbonate species have, also, been encountered on surfaces of metal oxides modified with alkali metal carbonates,[4,5] or at CO_2/alkali metal-modified metal oxide gas/solid interfaces.[6,7] Moreover, the activity of water-gas shift catalysts has been suggested to reside in dawsonite-like surface species.[8]

Applications of Dw and like compounds are diverse. The most prominent of these are the application as (i) a pollutant gas remover from emissions of coal-fired boiler systems,[9] (ii) a dry extinguisher of in-flight engine fuel leak fires,[10] (iii) a stabilizer for chlorine-containing polymers,[11] (iv) an effective ingredient in antacids,[12] (v) a parent material for transparent spinel[13] and YAG[14] ceramics, and (vi) a precursor for catalytic materials.[15] Admittedly, however, it is the latter application that has attracted our attention, whereby ultra high purity,[16] high-area thermally stable,[17] or metal-modified,[18] catalytic aluminas have been obtained via thermal decomposition of NH_4AlDw, BaAlDw, and BAlDw, respectively. Consistently, two favorable features have been observed. First, hydroxymetalocarbonates are generally thermally less stable than the corresponding metal carbonates.[4] Second, NH_4MDw is the appropriate precursor for pure M-oxides,

* Corresponding author. Fax: 0020862360833. E-mail: mizaki@link.net.
[†] Kuwait University.
[‡] Minia University.

(1) Railsback, L. B. *Carbonates Evaporites* **1999**, *14*, 1−20.
(2) Corazza, E.; Sabelli, C.; Vannucci, S. *Monatsh.* **1977**, *9*, 381−397.
(3) Hernandez, M. J.; Ulibarri, M. A.; Cornejo, J.; Pena, M. J.; Serna, C. J. *Thermochim. Acta* **1985**, *94*, 257−268.
(4) Iordan, A.; Zaki, M. I.; Kappenstein, C. *J. Chem. Soc. Faraday Trans.* **1993**, *89*, 2527−2536.
(5) Taylor, W. R. *Eur. J. Mineral.* **1990**, *2*, 547−563.
(6) Su, C.; Suarez, D. L. *Clays Clay Miner.* **1997**, *45*, 814−825.
(7) Kantschewa, M.; Albano, E. V.; Ertl, G.; Knözinger, H. *Appl. Catal.* **1983**, *8*, 71−86.
(8) Kochloefl, K. In *Handbook of Heterogeneous Catalysis*; Ertl, G., Knözinger, H., Weitkamp, J., Eds.; Wiley-VCH: Weinheim, 1997; Vol. 4, pp 1819−1831.
(9) Doyle, J. B.; Pirsh, E. A.; Downs, W. Eur. Pat. Appl. EP 87-307884, 19870907, 1988.
(10) Altman, R. L. *Prog. Astronaut. Aeronaut.* **1983**, *88*, 273−290.
(11) Wakagi, S.; Abe, C.; Sugawara, M. Jpn. Pat. Appl. JP 96-335863, 19961216, 1998.
(12) Zapryanova, A.; Dorkova, Z.; Paspaleeva, V. *Farmatsiya (Sofia)* **1987**, *37*, 14−19.
(13) Ikegami, T.; Li, J.-G.; Mori, T.; Lee, J.-H. Jpn. Pat. Appl. JP 2000-348042, 20001115, 2002.
(14) Ikegami, T.; Lee, G. G.; Mori, T.; Lee, J.-H. Jpn. Pat. Appl. JP 2000-86173, 20000327, 2001.
(15) Pitsch, I.; Gessner, W.; Brueckner, A.; Mehner, H.; Moehmel, S.; Uecker, D.-C.; Pohl, M.-M. *J. Mater. Chem.* **2001**, *11*, 2498−2503.
(16) Iga, T.; Furukawa, M.; Murase, Y. *Nagoya Kogyo Gijutsu Kenkyusho Hokoku* **1999**, *48*, 89−106.
(17) Giannos, M.; Hoang, M.; Turney, T. W. *Chem. Lett.* **1998**, *8*, 793−794.
(18) Pitsch, I.; Gessner, W.; Brueckner, A.; Pihl, M.-M. Ger. Pat. Appl. DE 99-19963599, 19991223, 2001.

10.1021/cm0519131 CCC: $30.25
Published on Web 11/23/2005

Table 1. General Methods of Dawsonite Preparation

method	phase composition[a]	reactants[b]	ref
I	g−l	$AlO_2^-{}_{(aq)} + Na^+{}_{(aq)} + CO_{2(g)}$	19
II	g−l	$AlO_2^-{}_{(aq)} + Na^+{}_{(aq)} + CO_3^{2-}{}_{(aq)}$ + urea ($\rightarrow CO_2\uparrow$)	20
III	g−s and s−s	$NaHCO_{3(s)} + Al(OH)_{3(s)} + CO_{2(g)}$	21
IV	l−l	$Al^{3+}{}_{(aq)} + Na^+{}_{(aq)} + HCO_3^-{}_{(aq)}$	22

[a] g = gas, l = liquid, s = solid. [b] aq = aqueous.

whereas other AMDw and BMDw are adequate precursors for alkalized and composite oxides, respectively.

Various methods have been devised for the preparation of Dw and like compounds. These may be classified, depending on the phase composition of the reactants, into the four general methods (I−IV) shown, as for example, for the preparation of NaAlDw in Table 1. In method-I,[19] pure Al metal strips are dissolved in a sodium hydroxide solution, and the yielding sodium aluminate solution is refluxed under a stream of CO_2 gas at constant temperature. In method-II,[20] a solution containing aluminum nitrate, sodium hydroxide, sodium carbonate, and urea is heated at ca. 90 °C. The urea slowly decomposes to release CO_2 gas, leading to a homogeneous precipitate of Dw. According to method-III,[21] a physical mixture of $NaHCO_3$ and $Al(OH)_3$ solid particles is calcined at 150−250 °C under CO_2 pressure. The solid-state reaction undertaken in this method is $NaHCO_{3(s)} + Al(OH)_{3(s)} = NaAlCO_3(OH)_{2(s)} + H_2O\uparrow$. Method-IV[22] involves a slow addition of an aqueous solution of $AlCl_3$ onto an aqueous solution of $NaHCO_3$ with vigorous stirring. The resulting gel is hydrothermally treated at a given temperature until complete formation of NaAlDw.

In the present investigation, preparation of NH_4MDw was attempted for M = Al, Cr, or Fe, using method-IV (Table 1). The basic objective was 2-fold: (i) to find optimal hydrothermal conditions for the preparation of NH4MDw and (ii) to examine the feasibility of dawsonites thus obtained as precursors for the thermal genesis of catalytic-grade, pure M(III)-oxides. Method-IV was preferred due to the fact that the particle size of the obtained dawsonite is largely dependent on, namely, two of the hydrothermal treatment variables: the pH and temperature.[22] A range of bulk and surface analytical techniques were applied to verify the dawsonite formation, and to assess properties of the oxides therefrom derived.

Experimental Section

Synthesis Method and Reagents. Synthesis of $NH_4M(CO_3(OH)_2$ (*denoted* NH_4MDw), where M stands for Al, Cr, or Fe, was attempted following the method reported by Wen et al.[22] Accordingly, a 250-mL aliquot of 0.1 M aqueous solution of $M(NO_3)_3 \cdot 9H_2O$ (99−99.9% pure Aldrich products) was added slowly to an equal volume of 1.25 M aqueous solution of NH_4HCO_3 (99% pure Aldrich product) while being continuously stirred at room temperature (RT). The pH value of the mixture was maintained constant (±0.1) at either of the following values: 8, 9, 10, and 11, using NH_4OH solution (25% Aldrich product). The gel thus obtained was hydrothermally treated at various temperatures (75−135 °C), for 24 h, inside a glass-lined, stainless steel autoclave (model 3870 EP, Tuttnauer Europe C.V.). Then, the slurry was removed, filtered, and washed several times with distilled water and ethanol. The white-, blue-, and brown-colored solid residues obtained, respectively, using Al-, Cr-, or Fe-nitrate, were dried at 100 °C for 24 h. For simplicity, the products are discerned below by the temperature and pH values applied. For instance, NH_4MDw9-75 means the product obtained at pH = 9 and 75 °C, whereas NH_4MDw11-135 signifies that obtained at pH = 11 and 135 °C. The products were kept dry over self-indicating silica gel.

Characterization Methods and Techniques. Chemical composition of the various NH_4MDw products was determined by CHNO and atomic absorption spectrometry (AAS). The bulk crystalline and noncrystalline structures were elucidated by X-ray powder diffractometry (XRD) and infrared absorption spectroscopy (IR), respectively. The surface area and particle morphology were, respectively, measured by N_2 sorptiometry and scanning electron microscopy (SEM). The thermal stability was probed by thermogravimetry (TG) and differential thermal analysis (DTA). Accordingly, the onset temperature of the thermal genesis of the corresponding M(III)-oxide was determined, and the oxides thus obtained were subjected to similar bulk and surface characterization studies.

AAS was carried out by means of a Perkin-Elmer model 5100 PC spectrometer. A solution of a 10-mg portion of the test sample in concentrated HNO_3 was sprayed as a fine mist into the flame-atomizer at 2100−2400 °C, employing air as the oxidant and C_2H_2 as the fuel. Analyses were conducted using the appropriate Hallow cathode light source. CHNO was conducted using Lecochns model 932. A 1.0-g portion of test sample was placed in a silver cell, and the combustion process was facilitated in an O_2/He gas mixture at 2000 °C. XRD was performed at RT using a D5000 Siemens diffractometer equipped with a source of Ni-filtered Cu Kα radiation (λ = 0.15406 nm). The diffractometer was operated at 40 kV and 30 mA, the data being acquired stepwise over the 2θ range 10−80° at a step size of 0.02°, a step time of 15 s, and a divergence slit of 1°. The data were manipulated using an on-line microcomputer. For crystalline phase identification purposes, an automatic JCPDS library search and match was conducted using a standard SEARCH and DIFFRAC software (Siemens Corp.), whereas for crystallite sizing, X-ray line broadening technique[23] and Scherrer formula[24] were implemented. IR spectra were measured for KBr-supported test samples (<1 wt %) over the frequency range 4000−400 cm^{-1} at a resolution of 5.2 cm^{-1} using a model 2000 Perkin-Elmer FT-IR spectrometer. TG and DTA analyses were carried out on heating, typically, a 8−10-mg portion of test samples, at 10 °C/min and 50 cm^3 of air/min, using a Shimadzu thermal system, model TGA-50H, equipped with a workstation for data acquisition and handling. Highly sintered α-Al_2O_3 (Shimadzu Corp.) was the thermally inert reference for DTA measurements. N_2 sorptiometry was performed (at −195 °C) with an automatic ASAP 2010 Micromeritics sorptiometer equipped with a degassing platform and an on-line data acquisition and handling system powered with BET-based[25] analytical software for the specific surface area (S_{BET}/m^2g^{-1}) determination. The N_2 gas was a 99.999% pure product of KOAC (Kuwait), and the test materials (500 ± 2 mg) were pre-degassed

(19) Cada, R. B. *Bull. Tokyo Inst. Technol.* **1971**, *9*, 23−31.
(20) Keenan, F. J.; Howatson, J.; Smith, J. W. *Energy Res. Abstr.* **1980**, *5*, Abstr. No. 25328.
(21) Altman, R. L.; Mayer, L. A.; Ling, A. C. U.S. Pat. Appl. US 81-317977, 19811103, 1982.
(22) Wen, Z. Y.; Yang, J. H.; Lin, Z. X.; Jiang, D. L. *Solid State Ionics: Materials and Devices*, Proc. 7th Asian Conf., Oct. 29−Nov. 4, 2000, Fuzhou, China; 2000; pp 79−83.
(23) Matyi, R. J.; Schwartz, L. H.; Butt, J. B. *Catal. Rev.-Sci. Eng.* **1987**, *29*, 41.
(24) Dann, S. E. *Reactions and Characterization of Solids*; The Royal Society of Chemistry: Cambridge, 2000; pp 64−65.
(25) Sing, K. S. W.; Rouquerol, J. In *Handbook of Heterogeneous Catalysis*; Ertl, G., Knözinger, H., Weitkamp, J., Eds.; Wiley-VCH: Weinheim, 1997; Vol. 2, pp 427−435.

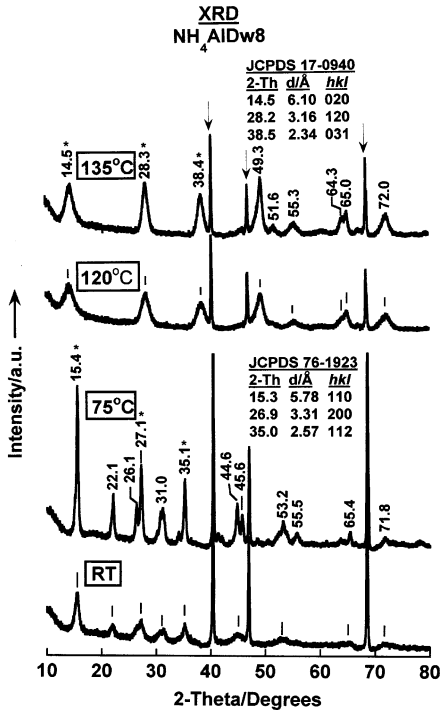

Figure 1. X-ray powder diffractograms for the hydrothermal product NH_4-AlDw obtained at pH = 8 as a function of the various temperatures indicated [↓ points out peaks due to the sample holder (Rt/Ph), * marks the relatively strongest three peaks, and the insets highlight the closest reference (JCPDS) data].

at 110 °C and 10^{-5} Torr for 3 h. SEM was conducted using a JSM-630 JEOL scanning electron microscope, operated at 30 kV. Test samples, spread in a thin layer over a double adhesive tape on a 10-mm aluminum stub, were sputter-coated with gold prior to examination.

Results and Discussion

Dawsonite Verification. To determine the optimal hydrothermal conditions for the synthesis of dawsonite-type $NH_4M(CO_3)(OH)_2$, for M = Al, Cr, or Fe, the products at various pH and temperature values were examined by XRD, IR, CHNO, and AAS analyses. Figure 1 compares XRD diffractograms obtained for NH_4AlDw products at pH = 8 as a function of the hydrothermal treatment temperature (RT-135 °C). It is obvious from the results that two different diffraction patterns are exhibited: (i) a typical $NH_4Al(CO_3)(OH)_2$ dawsonite pattern (JCPDS 76-1923)[26] shown by the products at <100 °C and (ii) an entirely different pattern, due to γ-AlOOH (JCPDS 17-0940),[26] shown by the products at >100 °C. The product at 100 °C showed drastic retrogression of the dawsonite pattern, without any indication for a substitute phase. IR spectra taken of NH_4AlDw8-75 and -135 (Figure 2) are consistent with the XRD results. The spectrum of the former material displays absorptions due to various bond vibrations of OH^- [νOH, at 3450 cm^{-1}; δOH, at 990 cm^{-1}],[27] NH_4^+ (νNH, at 3180, 3030, and 2850 cm^{-1}; δNH, at 1830 and 1730 cm^{-1}),[27,28] CO_3^{2-} [νC−O, at 1560(ν_3), 1460(ν_3), 1390(ν_3), 1110(ν_1), 860(ν_2), and 750 cm^{-1}(ν_4)],[27,29] and Al−O [νAl−O lattice vibrations, at 740, 630, and 490 cm^{-1}].[30] Closely similar IR spectral features have been reported for $NH_4Al(CO_3)(OH)_2$ by Serna et al.[27] On the other hand, the spectrum of the latter material is void, almost completely, of the characteristic absorptions of the NH_4^+ and CO_3^{2-} moieties of the NH_4AlDw, though it retains similar absorptions to those of lattice vibrations of Al−O bonds (at 740, 620, and 480 cm^{-1}). It displays, moreover, two absorptions assignable to νOH vibrations (at 3300 and 3090 cm^{-1}), and two absorptions at 3590 and 1070 cm^{-1} due, respectively, to stretching and bending vibrations of bent O−O−H.[31] According to Serna et al.,[32] the absorptions displayed for NH_4AlDw8-135 are characteristic for AlOOH species. The close similarity of the Al−O lattice vibrations of $NH_4Al(CO_3)(OH)_2$ and AlOOH (Figure 2) may sustain a mechanism put forward by Ishikawa et al.,[33] whereby formation of $AlO(OH)^-$ species in solution has been made necessary for the formation of AlDw compounds.

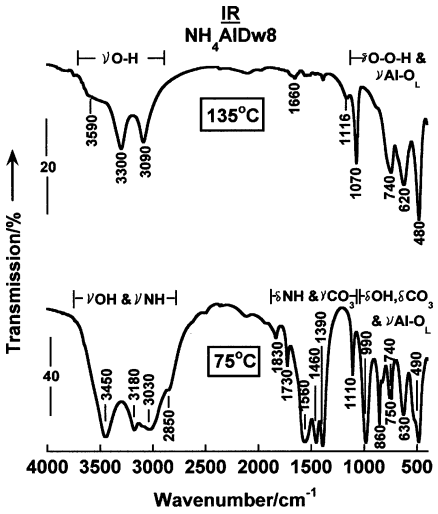

Figure 2. IR transmission spectra taken of NH_4AlDw8 obtained at the two hydrothermal treatment temperatures indicated.

To define the optimal pH range for $NH_4Al(CO_3)(OH)_2$ formation, hydrothermal products at pH >8 and 75 °C, namely, pH = 9, 10, and 11, were XRD-analyzed. The results obtained indicated a gradual intensification of the dawsonite diffraction peaks with the pH value. Figure 3 manifests the peak intensification, comparing the XRD patterns exhibited by the products at pH = 8 and 11, and 75 °C [both diffractograms are plotted to the same abscissa scale, and both test materials were of comparable amounts]. Upon further pH increase to 12, the product (at 75 °C) was rendered poorly crystalline to XRD. We find this result in line with findings of an exhaustive investigation of the solution chemistry leading to dawsonite formation, which confine the optimal pH range to >10 and <12.[33] The interpretation brought about[33] has been based on the fact that the solution equilibria $HCO_3^- \leftrightarrow CO_3^{2-}$ and $AlO(OH)_2^- \leftrightarrow Al(OH)_4^-$

(26) International Center for Diffraction Data, 12 Campus Boulevard, Newton Square, PA 19073−3273.
(27) Serna, C. J. S.; Garcia-Ramos, J. V.; Pena, M. J. *Spectrochim. Acta* **1985**, *41A*, 697−702.
(28) Nakamoto, K. *Infrared Spectra of Inorganic and Coordination Compounds*; Wiley-Interscience: New York, 1970; pp 106−108.
(29) Busca, G.; Lorenzelli, V. *Mater. Chem.* **1982**, *7*, 89.
(30) Frueh, A. J., Jr.; Golightly, J. P. *Can. Miner.* **1967**, *34*, 51−56.
(31) In ref 28, pp 88−91.
(32) Serna, C. J.; Rendon, J. L.; Iglesias, J. E. *Spectrochim. Acta* **1982**, *38A*, 797−802.
(33) Ishikawa, H.; Kwon, S. W.; Kim, B. H. *Memoirs School Sci. Eng., Wased Univ.* **1971**, No. 35.

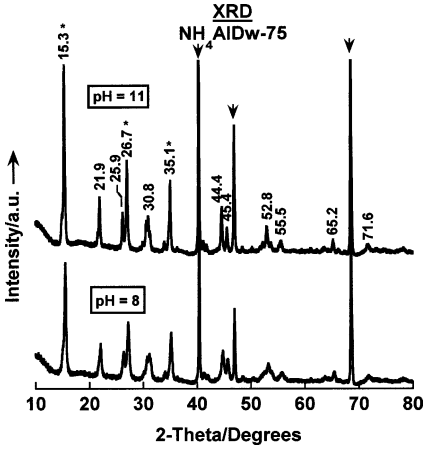

Figure 3. X-ray powder diffractograms for NH_4AlDw obtained at 75 °C as a function of the pH values indicated. [↓ and * significances are as in Figure 1].

are shifted to the left (i.e., in favor of HCO_3^- and $AlO(OH)_2^-$) at pH < 12. Thus, a reaction similar to that proposed[33] for formation of NaAlDw may be depicted for NH_4AlDw in the following equation:

$$NH_4^+ + AlO(OH)_2^- + HCO_3^- \rightarrow NH_4Al(CO_3)(OH)_2 + OH^-$$

Similar attempts to prepare Dawsonite-type compounds for Cr and Fe, under various hydrothermal conditions (RT-135 °C and pH = 8−12), led to the formation of the following compounds: $NH_4CrDw11$-100 and $NH_4FeDw11$-75. Hence, both compounds yielded similarly at pH = 11 and the low-temperature regime 75−100 °C. XRD patterns obtained for these two compounds are compared to that exhibited by $NH_4AlDw11$-75, i.e., $NH_4Al(CO_3)(OH)_2$, in Figure 4. The comparison reveals the following: (i) both compounds are far more less crystalline than AlDw, (ii) the detectable diffraction peaks displayed (at $2\theta = 15.4°$, 27.1°, and 34.9°) in the diffractogram of $NH_4CrDw11$-100 correspond satisfactorily to the strongest three peaks (at $2\theta =$ 15.3°, 26.7°, and 35.1°) of the dawsonite $NH_4Al(CO_3)(OH)_2$, and (iii) the detectable peaks (at $2\theta = 33.3°$, 36.3° and 54.1°) for $NH_4FeDw11$-75 do not correspond to those characteristic for AlDw, but rather to those filed either for α-Fe_2O_3 (JCPDS 84-0311)[26] or for the oxyhydroxide $Fe_{1.833}(OH)_{0.5}O_{2.5}$ (JCPDS 76-0182),[26] both being of rhombohedral structure. These results are corroborated by the IR spectra taken of the three test compounds, compared in Figure 5. The resemblance between the IR spectra of $NH_4AlDw11$-75 and $NH_4CrDw11$-100 is quite obvious since both spectra exhibit analogous sets of absorptions over the νOH and νNH frequency region (at <2800 cm^{-1}), the δNH and νCO_3 region (at 1850−1090 cm^{-1}), and the δOH, νCO_3, and νM−O region (at 1000−440 cm^{-1}). This sustains the XRD results in indicating that $NH_4CrDw11$-100 assumes a poorly crystalline dawsonite-type $NH_4Cr(CO_3)(OH)_2$ structure, whereas the entirely different IR absorption features observed for $NH_4FeDw11$-75 (Figure 5) display two broad, strongly overlapping νOH absorptions at 3400 and 3170 cm^{-1}, two weak, but distinct, absorptions at 1620 and 1380 cm^{-1} due, respectively, to δOH of water molecules and νNO_3^- of surface nitrate impurity

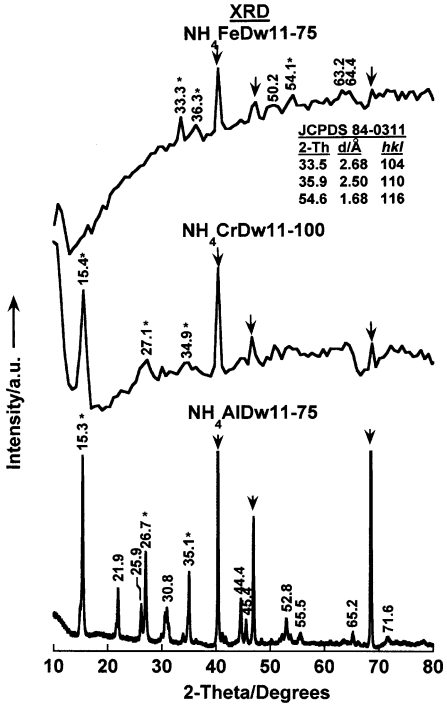

Figure 4. X-ray powder diffractograms for the hydrothermal products $NH_4CrDw11$-100 and $NH_4FeDw11$-75, whereas that of $NH_4AlDw11$-75 is given for comparison purposes. The top two diffractograms were mildly smoothed to improve the signal-to-noise ratio.

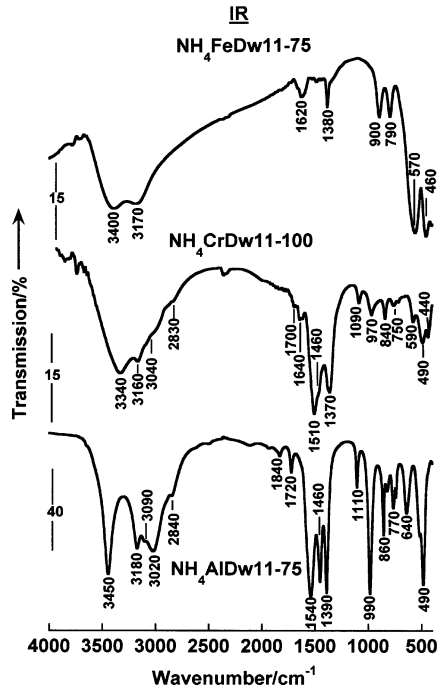

Figure 5. IR transmission spectra taken of the indicated hydrothermal products.

species, two sharp bands at 900 and 790 cm^{-1}, and two very strong absorptions at 570 and 460 cm^{-1}. The latter two absorptions occur at frequencies very close to those (570−60 and 460−50 cm^{-1}) reported for νFe(III)−O lattice vibrations of F(III)-oxides or oxyhydroxides.[34]

Elemental analysis results and chemical compositions therefrom derived for the three products obtained under the observed favorable hydrothermal conditions are given in Table 2. When compared to the empirical formula ($C_1H_6N_1O_5$-

Table 2. Elemental Analysis Results and Chemical Compositions Therefrom Derived for the Hydrothermal Treatment Products

product	C[a]/%	H[a]/%	N[a]/%	O[b]/%	M[c]/ppm	found composition[d]
NH_4-AlDw11-75	7.9525	4.5431	8.7970	61.253	157075	$C_{1.14}H_{7.82}N_{1.07}O_{6.44}Al_{1.00}$
NH_4-CrDw11-100	4.7011	3.7951	5.6129	57.344	286407	$C_{0.71}H_{6.72}N_{0.73}O_{6.49}Cr_{1.00}$
NH_4-FeDw11-75	0.6516	1.4399	0.3267	36.319	612623	$C_{0.05}H_{1.31}N_{0.02}O_{2.06}Fe_{1.00}$

[a] CHNO-determined mass %. [b] Determined by difference (in mass %). [c] AAS-determined; M = Al, Cr, or Fe. [d] Determined in gram-atom proportions relative to a gram-atom of the metal.

Al_1) corresponding to the molecular formula $NH_4Al(CO_3)(OH)_2$ expected for NH_4AlDw11-75, the derived formula, $C_{1.14}H_{7.82}N_{1.07}O_{6.44}Al_{1.00}$, conveys very close atomic proportions for all of the elements detected, except for H and O. The observed extra-formula amounts of these two elements; viz., $H_{1.82}O_{1.44}$, may originate from minority amounts of unconverted AlOOH species and/or molecular water. A similar handling of the results obtained for NH_4CrDw11-100 (Table 2) also reveals that the observed empirical formula, $C_{0.71}H_{6.72}N_{0.73}O_{6.49}Cr_{1.00}$, accounts approximately for a hydrated dawsonite-type molecular formula, $NH_4Cr(CO_3)(OH)_2 \cdot 0.5H_2O$. The slight discrepancies between the observed and proposed compositions, particularly over the oxygen proportion, may be ascribed to the poor crystallinity of the material, as well as the known tendency of chromium compounds toward excess oxygen uptake.[35] On the other hand, the observed empirical formula, $C_{0.05}H_{1.31}N_{0.02}O_{2.06}Fe_{1.00}$, for NH_4FeDw11-75 discloses that the minute amounts of C and N are due to impurity species, and that the bulk formula is obviously closer to corroborate the molecular formula of the hydrated oxyhydroxide $Fe_{1.83}(OH)_{0.5}O_{2.5} \cdot H_2O$ than that of the hydrated oxide $Fe_2O_3 \cdot H_2O$. Thus, NH_4-FeDw11-75 is not a dawsonite-type compound, but rather a dawsonite-precursor compound. This is in the sense that the implied oxyhydroxide formula is almost equivalent to the simpler $FeOOH \cdot xH_2O$ formula. Hence, the two IR bands observed at 900 and 790 cm^{-1} for NH_4FeDw11-75 (Figure 5) are most likely due, respectively, to vibrations of O−O and O−O−H bonds. These results may underline the importance of metal oxyhydroxide species as a precursor not only for formation of AlDw but also for CrDw and FeDw. As previously reported,[33] it is the pH-controlled competition between the formation, and subsequent precipitation, of the metal oxyhydroxide and dawsonite that dictates the synthesis course to the latter compound.

Thermal Decomposition Events. TG and DTA curves, compared in Figure 6, monitor a single, strong endothermic mass loss (ML) process for NH_4AlDw11-75 (T_{max} = 219 °C; overall ML = 60.9%) while being heated in a dynamic atmosphere of air at RT-1000 °C. It is shown to involve two kinetically different steps: (i) a very rapid step at 190−258 °C, involving most of the overall ML (54%), and (ii) then a very slow step at 250−1000 °C, increasing the ML up to 60.9%. These results are close to the reported[3] TG and DTA

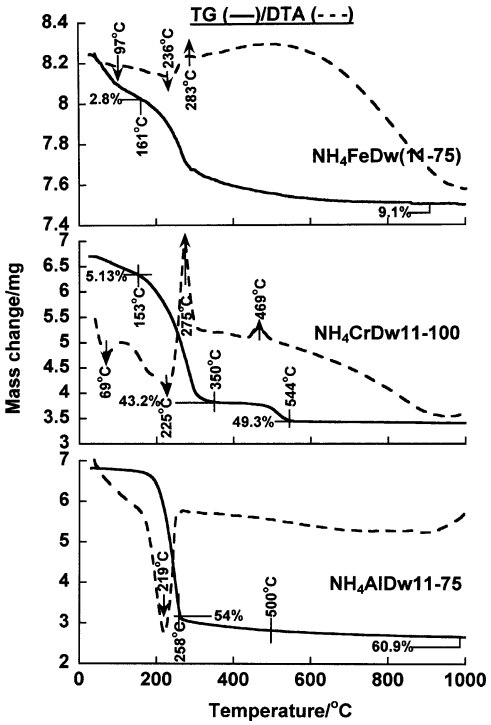

Figure 6. TG and DTA curves obtained (at 10 °C/min and 50 cm^3 air/min) for the indicated hydrothermal products.

results for $NH_4Al(CO_3)(OH)_2$ decomposition according to the following, strongly overlapping reaction steps:

$$6NH_4Al(CO_3)(OH)_2 \rightarrow 4CO_2 + 9H_2O + 6NH_3 \; [T_{max} = 230\ °C;\ ML = 52.8\%] \quad (1)$$

$$+ Al_6O_7(CO_3)_2 \rightarrow 3Al_2O_3 + 2CO_2 \; [T = 350-500\ °C;\ ML = 7.8\%] \quad (2)$$

Thus, the observed rapid, strong mass loss step (observed ML = 54%) should, most likely, involve the decomposition of $NH_4Al(CO_3)(OH)_2$ into the oxycarbonate $AlO_{1.16}(CO_3)_{0.33}$ (expected ML = 52.8%), whereas the following much slower mass loss step (observed ML = 6.9%) should involve the decomposition of the oxycarbonate into the oxide $AlO_{1.5}$ (Al_2O_3; expected ML = 7.8%). The fact that the observed overall ML (= 60.9%) is slightly higher than the expected one (60.6%) may be ascribed to the presence of a minute amount of weakly held water molecules. On the other hand, these results are quite supportive of the XRD, IR, and elemental analysis results (Table 2) in confirming that NH_4-AlDw11-75 is, indeed, the dawsonite $NH_4Al(CO_3)(OH)_2$, which decomposes almost completely, via an intermediate aluminum oxycarbonate, giving pure Al_2O_3 at ≥500 °C.

TG and DTA results obtained for NH_4CrDw11-100 (Figure 6) monitor a multistep decomposition process: (i) two overlapping endothermic ML steps at <153 °C, effecting a mass loss of ca. 5.13%, (ii) a strong, endothermic, fast ML-step (T = 153−350 °C; ML = 43.2−5.13 = 38.1%), intersected by a strong exothermic process (T_{max} = 275 °C), (iii) a mass-invariant exothermic process (T_{max} = 469 °C), and (iv) a fast ML step (=49.3−43.2 = 6.1%), commencing in the immediate vicinity of the preceding exothermic process and ceasing at 544 °C. In the absence of thorough physicochemical analyses of the intermediate decomposition steps

(34) Gadsden, J. A. *Infrared Spectra of Minerals and Related Inorganic Compounds*; Butterworths: London, 1975; pp 44−46.
(35) Rode, T. V. *Oxygen Compounds of Chromium Catalysts*; Izd. Akad., Nauk SSSR: Moscow, 1962; pp 63−69.

and products, which is the case here, it is practically impossible to define the solid-state chemical reactions occurring. The complexity of high-temperature solid-state reactions of Cr(III) compounds is known to be due to a redox cycle (Cr(III) → Cr(IV−VI) → Cr(III)) conceded by Cr(III) dwelled in noncrystalline or less ordered transitional state structures when heated at 200−400 °C in oxidizing atmospheres.[35−37] This redox behavior is, often, manifested in DTA curves of Cr(III) compounds by an exotherm, at 200−300 °C, indicative of the oxidation process (Cr(III) → Cr(IV−VI)),[34−36] and another exotherm, at 400−500 °C, indicative of a crystallization accompanying the subsequent reduction process (Cr(IV−VI) → Cr(III)).[35−37] Thus, the exotherm displayed for $NH_4CrDw11\text{-}100$ at 275 °C (Figure 6) is most likely that indicating the oxidation of Cr(III), occurring during the decomposition of the compound, whereas the exotherm observed at 469 °C (Figure 1) is that indicating crystallization of the reduction Cr(III) product. Bearing in mind these considerations, the following decomposition course may be depicted for $NH_4CrDw11\text{-}100$ ($=NH_4Cr(CO_3)(OH)_2{\cdot}0.5H_2O$; Table 2):

$$6NH_4Cr(CO_3)(OH)_2{\cdot}0.5H_2O \rightarrow 3H_2O\ [T \leq 153\ ^\circ C;\ \text{expected ML} = 5.2\%] \quad (3)$$

$$+ 6NH_4Cr(CO_3)(OH)_2 + 1.5O_2 \rightarrow 4CO_2 + 6NH_3 + 9H_2O\ [T = 153-350\ ^\circ C;\ \text{expected ML} = 42.4\%] \quad (4)$$

$$+ Cr_6O_{10}(CO_3)_2 \rightarrow 3Cr_2O_3 + 2CO_2 + 1.5O_2\ [T = 469-544\ ^\circ C;\ \text{expected ML} = 22.9\%] \quad (5)$$

It is obvious that the expected mass losses for the dehydration (5.2%) step (eq 3) and the oxidative decomposition (42.4%) step (eq 4) are very close to the observed ones (5.13 and 43.2%), respectively. In contrast, the expected ML (=22.9%) for decomposition of the intermediate oxycarbonate to the onset of formation of Cr_2O_3 is much higher than the observed one (=49.3−43.2 = 6.1%; Figure 6). Although this fact may shed a large amount of doubt on the nature of the intermediate, whether it is an oxycarbonate solely of Cr(IV), as suggested, or it is of a higher oxidation state of Cr, or a mixture of them, or alternatively an entirely different oxygen-rich species of Cr(III−VI), the expected overall ML (= 56.0%), as per the following equation, is not that much higher than the observed total ML (=49.3%):

$$6NH_4Cr(CO_3)(OH)_2{\cdot}0.5H_2O + 1.5O_2 \rightarrow 3Cr_2O_3 + 6CO_2 + 12H_2O + 6NH_3 + 1.5O_2 \quad (6)$$

TG and DTA results obtained for $NH_4FeDw11\text{-}75$ (Figure 6), which has been suggested by elemental analyses to assume the non-dawsonitic composition $Fe_{1.83}(OH)_{0.5}O_{2.5}{\cdot}H_2O$; i.e., $FeOOH{\cdot}xH_2O$, resolve two ML steps: (i) an initial step, leading to 2.8% ML completed near 161 °C and (ii) a subsequent ML step, mounting the total ML up to 9.1% near 900 °C. The second ML step is initially rapid and slows down significantly toward the end. It is shown to involve two strongly overlapping endo- and exothermic processes at 236 and 283 °C, respectively. These effects are shown to be broad and ill-defined (Figure 6). Considering the formula $FeOOH{\cdot}xH_2O$ for $NH_4FeDw11\text{-}75$, an overall decomposition into Fe_2O_3 would result in ca. 10% ML, which is slightly higher than the observed overall ML (=9.1%). The slight ML difference may be attributed to the exothermic contribution to the second ML step, which is due, most likely, to a minute oxidation to compensate for the nonstoichiometric nature of the material. Without going into any further details, for which we have no experimental justification, $NH_4FeDw11\text{-}75$ is, thus, shown to assume a non-dawsonitic composition, but rather an oxyhydroxide composition ($FeOOH{\cdot}xH_2O$), i.e., a dawsonite−precursor composition. It decomposes almost completely into Fe_2O_3 at ≥600 °C.

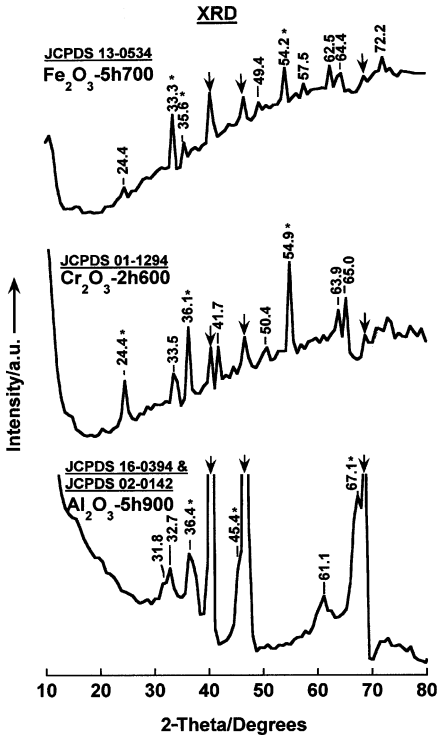

Figure 7. X-ray powder diffractograms for the indicated calcination yields of the test hydrothermal treatment products. The diffractograms were mildly smoothed to improve the signal-to-noise ratio.

The above TG and DTA results are supportive of the XRD, IR, and elemental analysis results in confirming that the hydrothermal products of Al and Cr assume ammonium dawsonite-type compositions, but that of Fe does not. Moreover, they determine temperature regimes over which these compounds decompose completely into the corresponding M_2O_3 oxide. Accordingly, they were calcined at different high temperatures for various time durations, and XRD, N_2 sorptiometry, and SEM were employed to characterize the calcination products. The following section sets out the results obtained for the calcination product of $NH_4AlDw11\text{-}75$ at 900 °C for 5 h (*denoted* Al_2O_3-5h900), $NH_4CrDw11\text{-}100$ at 600 °C for 2 h (Cr_2O_3-2h600), and $NH_4FeDw11\text{-}75$ at 700 °C for 5 h (Fe_2O_3-5h700).

High-Temperature Decomposition Products. Figure 7 compares the XRD patterns exhibited by the decomposition products Al_2O_3-5h900, Cr_2O_3-2h600 and Fe_2O_3-5h700. The diffraction peaks observed for Al_2O_3-5h900 are very close to the standard data filed for δ-Al_2O_3 in JCPDS 02-0142

(36) Zaki, M. I.; Fouad, N. E. *Thermochim. Acta* **1985**, *95*, 73.
(37) Zaki, M. I.; Fahim, R. B. *J. Therm. Anal.* **1986**, *31*, 825.

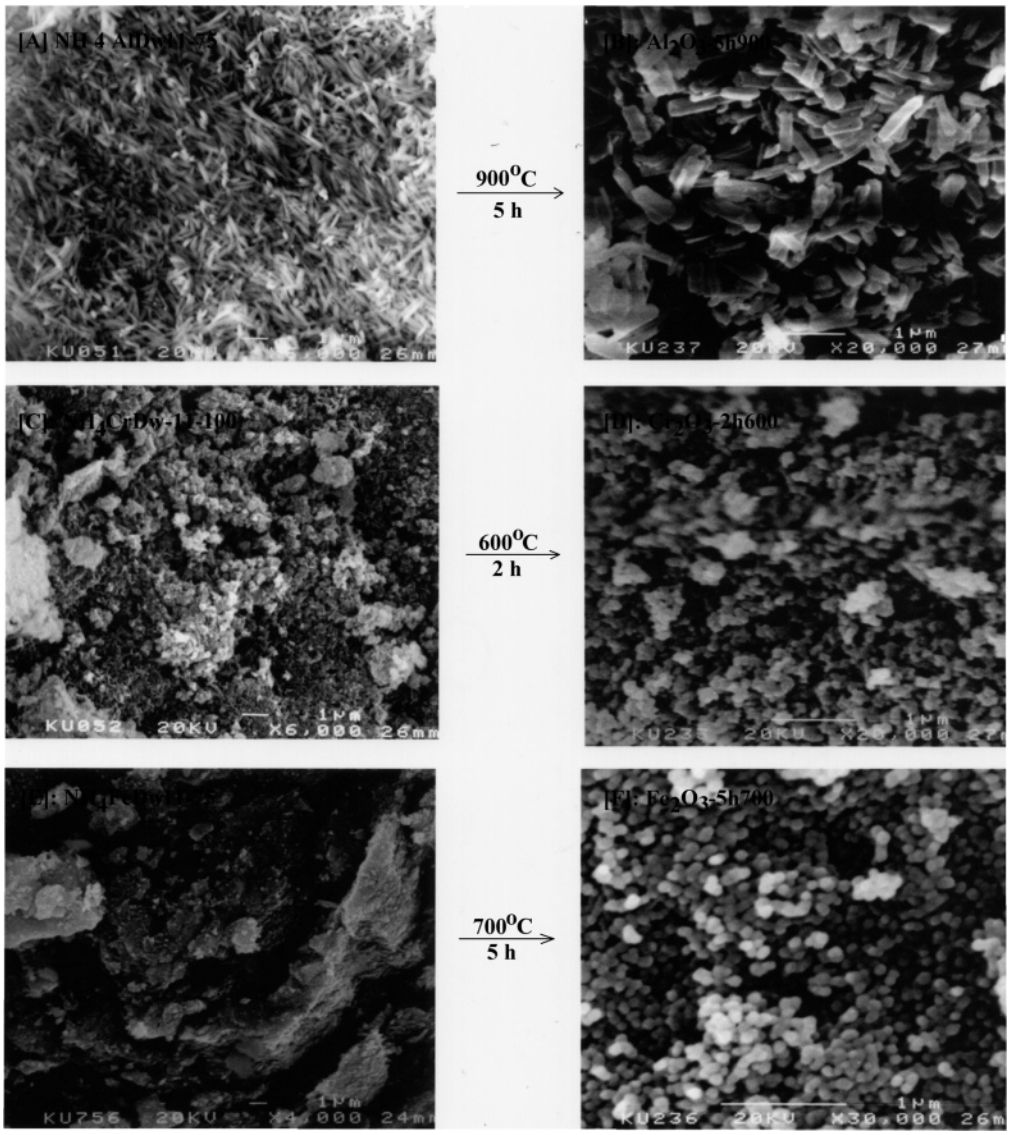

Figure 8. Scanning electron micrographs for the indicated hydrothermal treatment products [A, C, and D] and their corresponding calcination products [B, D, and F], respectively.

Table 3. Average Crystallite Size (D)[a] and Specific Surface Area (S_{BET})[b]

material	$D/\pm 2$ nm	$S_{BET}/\pm 3$ m^2 g^{-1}
$NH_4AlDw11\text{-}75$	48	38
Al_2O_3-5h900	10s[c]	146
$NH_4CrDw11\text{-}100$	8[a]	263
Cr_2O_3-2h600	36	32
$NH_4FeDw11\text{-}75$	12[c]	99
Fe_2O_3-5h700	56	13

[a] It was determined by averaging values derived from XRD peak breadth at half-maximum for the strongest three peaks, implementing Scherrer formula.[24] [b] It was determined by BET analysis of N_2 adsorption data. [c] These data are accurate to within ±4 nm.

and/or γ-Al_2O_3 in JCPDS 16-0394. The obvious weakness and broadness of the peaks account for an overall weak crystallinity and small crystallite sizes. Consistently, the average crystallite size derived from the peak breadth at half-maximum is almost one-fifth (10 nm) of that similarly determined for the parent $NH_4AlDw11\text{-}75$ (48 nm), Table 3. Consequently, the specific surface area determined for Al_2O_3-5h900 (146 m^2/g) is almost 4 times that (38 m^2/g) determined for the parent compound, Table 3. Bearing in mind the high calcination temperature applied to genesize the oxide (900 °C), the high accessibility of the surface brings into prominence the feasibility of the parent $NH_4Al(CO_3)(OH)_2$ as a precursor for catalytic-grade ($\gamma+\delta$)-Al_2O_3.

Similarly weak XRD diffraction peaks, occurring at comparable 2θ values (Figure 7), are exhibited by Cr_2O_3-2h600 and Fe_2O_3-5h700. Matching with standard XRD data files,[26] the diffraction pattern exhibited by the former product is very close to that filed for α-Cr_2O_3 in JCPDS 01-1294, whereas the pattern exhibited by the latter product is almost identical to that filed for α-Fe_2O_3 in JCPDS 13-0534. Despite their similar crystalline structure (corundum structure), the former product is of smaller average crystallite size, and hence higher specific surface area, than the latter product (Table 3). When related to the nature of the parent compound, these results also stress the feasibility of the dawsonite-type composition of the parent material (only of Cr_2O_3-2h600) in producing oxides of relatively higher surface accessibility.

Figure 8 compares scanning electron micrographs obtained for the parent $NH_4AlDw11\text{-}75$, $NH_4CrDw11\text{-}100$, and $NH_4FeDw11\text{-}75$ and their calcination products Al_2O_3-5h900, Cr_2O_3-2h600, and Fe_2O_3-5h700, respectively. The micrograph

of the parent NH_4AlDw11-75 images loose lath-like particles that are 800−1000 nm long and 200−300 nm wide (Figure 8A), whereas the calcination product Al_2O_3-5h900 is shown to consist of 400−500 nm long and 100−150 nm wide cylindrical particles (Figure 8B). The micrograph of NH_4-CrDw11-100 (Figure 8C) shows loose and aggregated small fibrous particles that are 500−600 nm long and 150−200 nm wide, whereas the calcination product Cr_2O_3-2h600 is visualized to consist of loose and aggregated spherical particles of an average size in the range 100−150 nm (Figure 8D). On the other hand, the parent NH_4FeDw11-75 is shown to consist of a few μm thick and bride clumps (Figure 8E), whereas the calcination product Fe_2O_3-5h700 is shown to consist of loose, uniform spherical particles of an average size in the range 90−120 nm (Figure 8F). The fact that SEM-determined average particle sizes are generally much larger than the corresponding XRD-determined average crystallite sizes (Table 3) of either of the test materials implies that the material particles are agglomerates of single crystallites.

Conclusion

The above presented and discussed results may help in drawing the following conclusions:

1. The optimal hydrothermal conditions for the preparation of dawsonite-type $NH_4M(CO_3)(OH)_2$ compound, for M = Al or Cr, are furnished at pH > 10 and pH < 12 and temperature $\leq$100 °C.

2. Aqueous $MO(OH)_2^-$ and HCO_3^- are the most probable ionic species established, under these conditions, in the preparation course of the dawsonite-type compounds.

3. Formation of sparingly soluble oxyhydroxide species interrupts the synthesis of $NH_4Fe(CO_3)(OH)_2$, leading eventually to the precipitation of FeOOH compound.

4. Calcination of dawsonite-type $NH_4M(CO_3)(OH)_2$ compounds results in the formation of catalytic-grade M_2O_3 oxides.

Acknowledgment. The financial support facilitated by the College of Post-graduate Studies, and the excellent technical assistance found at the Science Analytical Facility (SAF) and Electron Microscopy Unit of the Faculty of Science of Kuwait University are highly appreciated.

CM0519131